

TWELFTH EUROPEAN ROTORCRAFT FORUM

PAPER N° 23

A PRESCRIBED RADIAL CIRCULATION DISTRIBUTION OF
A HOVERING ROTOR BLADE

by

C. MARESCA ; D. FAVIER ; M. NSI MBA

Institut de Mécanique des Fluides de Marseille
UM 34 du C.N.R.S.
1, rue Honnorat - 13003 Marseille - FRANCE

September 22 - 25 1986

Garmisch - Partenkirchen - GERMANY

A PRESCRIBED RADIAL DISTRIBUTION CIRCULATION
OF A HOVERING ROTOR BLADE

by



C. MARESCA, D. FAVIER, M. NSI MBA

Institut de Mécanique des Fluides, UM 34 du CNRS

1, rue Honnorat, 13003 MARSEILLE

(France)

Abstract

-

A prescribed radial distribution circulation has been deduced from new experimental results obtained on hovering rotor blades. The synthesized empirical law of circulation is used as input data of an iterative numerical code predicting the wake geometry, the rotor in flow and airloads. Compared to the previous code using a prescribed distribution of induced velocities, improvements concerning running time and precision on wake characteristics have been obtained. Moreover, it has been shown that, in the case of highly non linear twisted blade, the code becomes efficient when introducing the experimental values of the bound circulation along the blade as input data. Particularly, the wake geometry given by the code shows a good agreement with experiments.

NOMENCLATURE

b	: Number of blades
c	: Local blade chord, (m)
C_T	: Rotor thrust coefficient ($C_T = T/\rho (\Omega R)^2 \pi R^2$)
Γ	: Bound circulation on the blade, (m^2/s)
γ_n	: Coefficient of the circulation law given by Eq. (1)
ξ	: Reduced blade radius, ($\xi = r/R$)
n	: Blade rotational frequency (r.p.s.)
ψ	: Blade azimuthal angle, (deg)
ϕ	: Polar angle defined by Eq. (1)
r	: Radial distance from the axis of rotation, (m)
r_0	: Root cut out, (m)
R	: Rotor radius, ($R = 0,75$ m)
T	: Rotor thrust (N)
θ_v	: Local blade twist angle (deg)
θ	: Blade pitch angle at $\xi = 0.75$, (deg)
ω, Ω	: Angular rotational speed, $\Omega = 2 \pi n$, (rad/sec)
u, v, w	: Velocity components, (m/s).

1. INTRODUCTION

The improvement of the rotorcraft hover performance is closely linked to the development of several numerical procedures presently predicting the wake geometry, the rotor inflow and airloads. These codes (see for instance references 1, 2, 3) are generally based on iterative process resulting in free wake calculation techniques deduced from a prescribed wake modelled from experiments. The calculated results are more or less precise or time consuming according to more or less realistic input data, like : wake geometry, induced velocities, etc.

Moreover, most of the existing codes use an iterative procedure to determine the radial bound circulation of the blade. That means : as far from the exact solution is the initial and prescribed value of circulation, as long is the calculation procedure.

A precise measurement of the radial circulation along an helicopter blade has been lacking as long as the use of the laser velocimeter was introduced⁽⁴⁾⁽⁵⁾ and made possible a non intrusive investigation of the bound circulation distribution by avoiding probe interference and eventual encounters blade-probes when measurements are performed close to the blades.

The present paper aims to carry out a prescribed radial distribution circulation blade of a hovering rotor deduced from several experiments performed on 2, 3 and 4 bladed rotors for different values of the collective pitch angles. The twist of the blades is linear and the planform rectangular. The synthesized empirical law of circulation becomes an input of the numerical code already developed, resulting in a reduction from three iterative loops in one loop.

Results given by this new procedure are in better agreement with experiments, concerning particularly velocities in the wake and tip vortex paths. Moreover, discrepancies between experiments and calculations obtained with the previous code on highly non linear twisted blades, are minimized when a realistic law of bound circulation is used as input in the calculation code.

2. EXPERIMENTAL RESULTS OF RADIAL DISTRIBUTION CIRCULATION,

Many experiments concerning tip vortex paths, distribution of velocities in the wake, visualizations, overall forces have been performed at IMFM on several rotors (see figure 1) operating in hovering flight. Particular attention has also been paid to the determination of the bound circulation along the blade.

The technique used to measure the circulation is detailed in reference 5 and consists in measuring the variation of the tangential velocity component with the phase by use of a 2D laser velocimeter operating in backscattering mode. The measurement is made on the upper and lower side of the rotating plane, as close as possible to the blades ; the circulation is then deduced by integrating the velocity profiles⁽⁵⁾. In order to point out a synthesized formula of radial circulation distribution, measurements have been extended to several rotors of different number of blades ($2 \leq b \leq 4$) and different pitch angle ($6^\circ \leq \theta \leq 10^\circ$).

The planform of the blade is rectangular and the twist is linear (rotor No. 7).

All the measured circulation distributions have been synthesized according to the following formula deduced from general Glauert series :

$$(1) \Gamma(\phi) = \sum_{n=1}^{10} \gamma_n \sin(n\phi)$$

where $\phi = \text{Arc cos} (2\xi - 1 - \xi_0 / (1 - \xi_0))$

with $\xi = \frac{r}{R}$; $\xi_0 = \frac{r_0}{R}$ (r : radial distance along the blade ;

R : blade radius ; r_0 = Root cut out)

and $\gamma_n = \gamma_n^1(\theta) b + \gamma_n^2(\theta) b^2 + \gamma_n^3(\theta) b^3$ ($1 \leq n \leq 10$)

where θ is the collective pitch angle , b the number of blades

$$\text{and } \gamma_n^j = \alpha_n^j \theta + \beta_n^j \theta^2 + \delta_n^j \theta^3 \quad 1 \leq j \leq 3$$

The table presented in figure 2 summarizes the values of

$$\alpha_n^j, \beta_n^j \text{ and } \delta_n^j \text{ corresponding to } b = 2, 3, 4 \text{ and} \\ \theta = 6^\circ, 8^\circ, 10^\circ.$$

As examples, figures 3, 4, 5, 6 show the fitting of formula (1) with experiments on three and four bladed rotors, for $\theta = 6^\circ, 8^\circ, 10^\circ$.

3. CALCULATION

Figure 7 shows the block-diagram of the "Lifting Line Aerospatiale Hovering Code" (3) improved by optimising the number of calculation points on the blade with respect to b , the tip vortex core size and the far wake geometry (figure 8). In the new code the model a) of figure 8 is replaced by model b) of figure 9. A near region is defined for $0 < \psi < 5\pi/b$, where the free wake calculation is achieved; for $5\pi/b < \psi < 10\pi/b$ corresponding to vortex instabilities observed experimentally, the tip vortices are supposed to have an helicoidal path of constant pitch. The far wake ($\psi > 10\pi/b$) is modelled by a semi-infinite circular cylinder of intensity $d\Gamma/dz$.

This improved code, as presented on figure 7, has been tested by comparison to experiments made on radial circulation distributions for a three-bladed rotor and for $\theta = 6^\circ, 8^\circ, 10^\circ$ (see figure 10).

It can be observed that the calculation is efficient, in particular when concerning the position and the amplitude of the maximum of circulation along the blade.

We can conclude that the code presented on figure 7 is a good one for linear twist and rectangular planform blades, as long as distribution of circulation along the blade and tip vortex paths are concerned. But velocities in the wake are not so well predicted and the value of θ when the calculation has converged is different from the real geometrical value.

The following table shows, as an example, the values of the pitch angle θ_{cal} obtained after convergence of the code in different cases, for a three bladed rotor :

θ	10°	8°	6°
θ_{cal}	$13,07^\circ$	$10,25^\circ$	$7,83^\circ$

Table 2

4. USE OF FORMULA (1) IN THE CODE

In order to avoid the variation of the general pitch angle during the convergence procedure, and obtain more accuracy in the distribution of the wake velocities, an improvement of the code (noted code 1) is proposed in the following way :

- at step 0 (see Fig. 7), prescribed induced velocities are replaced by the prescribed circulation distribution of formula 1. Loops 1 and 3 are then cancelled and the block-diagram is reduced to :

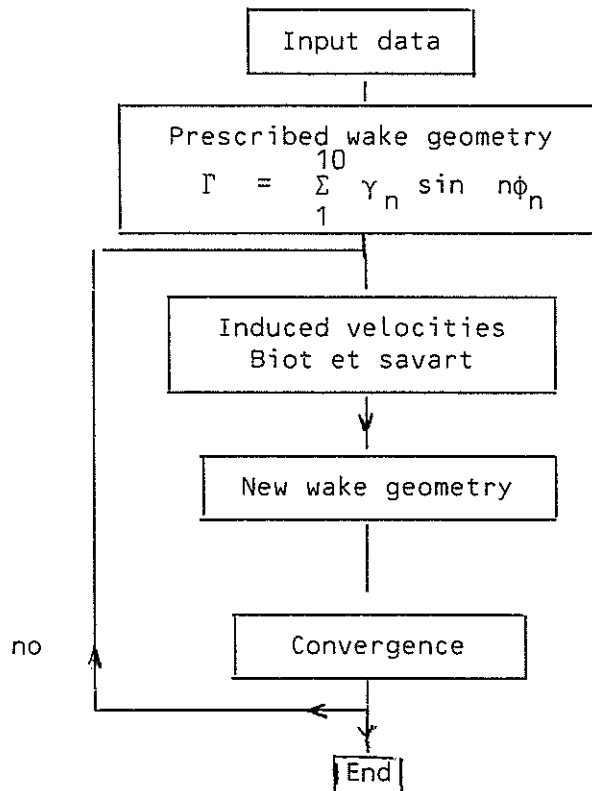


Table 3 : Modified calculation Code 2.

The running time of this new procedure (noted code 2) is reduced by a factor of 3. After convergence, the new distribution of circulation is calculated and compared to the prescribed circulation (formula 1) in the following way: The induced velocities (u and w) are calculated, after convergence of code 2, in the rotating plane by use of Biot et Savart law. The incidence is deduced for each radial position on the blade and the lift coefficient is given by 2-D steady polars of the blade profiles. The circulation is then deduced by Kutta-Joukowski law and the traction of the rotor, calculated by integrating the circulation along the blade, is compared to experimental values.

Table 4 is a summary of some typical results concerning rotor number 7 for $\theta = 6^\circ, 8^\circ, 10^\circ$ and $b = 3$ and 4.

θ	6°	8°	10°
b	4	3	3
$T_{\text{exp}} \text{ (N)}$	75	120	161
T_{calcul}	60	115	154

Table 4

The velocity components in the wake u, v, w have been calculated from codes presented in figure 7, and table 3, and compared to experiments performed by use of a laser velocimeter (see Ref.5). Comparisons were made in many cases of rotors (rectangular planform blades and linear twist) and several positions of Z/R in the wake.

Velocities are measured and computed in a fixed frame so that the fixed velocity profiles are changing with the value of the phase.

As examples, figures (11) to (20) present for different phases ψ , the variation with the radius distance along the blade of radial, tangential and axial velocity components. One axial plane ($Z/R = -0.015$) is considered and the results are relative to a four-bladed rotor No. 7 (see figure 1). On one hand, it can be seen that radial component is well predicted both by the two codes at $\psi = 36^\circ$ and $\psi = 45^\circ$ (figures 11,12) where experimental results show a smooth variation with r/R . On the other hand, experiments relative to $\psi = 18^\circ$ (figure 13) attest of a peak of velocity in the tip region, which is not predicted by code 1, and fairly corroborated by code 2.

Concerning the tangential components, figures (14) to (16) relative to $\psi = 36^\circ, 45^\circ, 81^\circ$ respectively show that the velocity level is low and less than 1 ms^{-1} . Both codes 1 and 2 are in good agreement with experiments.

Finally, the variations of axial components are presented on figures (17) to (20) for $\psi = 9^\circ, 63^\circ, 72^\circ$ and 81° . It can be observed that code 2 is efficient for describing peaks of velocity.

(as already mentioned on radial components), particularly when tip vortex is approaching the measurement point in the wake. In this case code 1 shows a failure, although it remains efficient in region where the velocity varies fairly with radial distance (see figure 18 relative to $\psi = 63^\circ$).

In conclusion, code 2 reduces running time, improves the velocity calculation in the wake, and has the best on code 1 to keep the collective pitch constant along the calculation.

5. EXTENSION OF CODE 2 TO HIGHLY NON LINEAR TWISTED BLADES

Rotor No. 3 in figure 1 has been tested experimentally and numerically (Code 1). The twist law is presented on the top of figure (21). Results of calculation by code 1 and by a lifting surface code (Ref. 6) are shown on the bottom of the figure concerning the radial distribution of circulation. Both codes use, as input data, a prescribed wake based on linear twist blade (Ref. 7), that induces discrepancies between calculations and experiments as it can be seen on figure (21). Moreover, comparison of calculated tip vortex path (dashed line in figure (22)) with experiments of reference (7) performed by hot wires (H.W.) and visualization (VISU) reveals an important misfit, particularly on the axial position Z/R of the vortices.

A tentative adaptation of code 2 has been made by introducing the experimental value of circulation. The results on tip vortex path are presented on figure (22) by a continuous line attesting a good modelisation as soon as the prescribed blade circulation is used.

6. CONCLUSION

From experiments performed on rectangular planform linear twisted blades, an attempt in improving and extending a free wake analysis for hovering rotors has been made in this study by use of a prescribed radial distribution of the circulation along the blade.

The prescribed law formulation has been carried out from several experiments of circulation previously performed and used as input in a new wake analysis code. Time convergence of this new code, requiring only one iterative loop versus 3 loops for the previous code, is reduced by a factor of 3. Moreover, the previous code requires changing the geometrical pitch angle during the convergence procedure, while the pitch angle remains constant in the new procedure.

It has also been shown that the calculation of velocity components in the wake have been significantly improved, particularly in the region of tip vortices. Peaks induced on axial and radial velocities by tip vortex lines are well predicted when compared to experimental results

The use of a prescribed circulation law has been extended with success to the case of a highly non linear twist which cannot be calculated by using the free wake analysis method usually used (due to the lack of

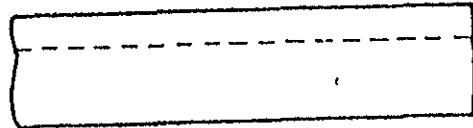
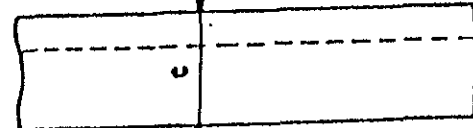
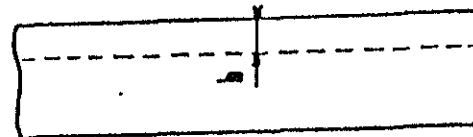
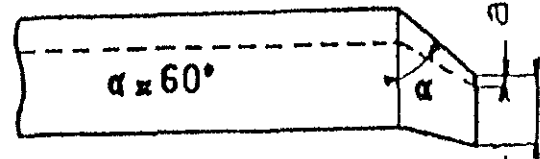
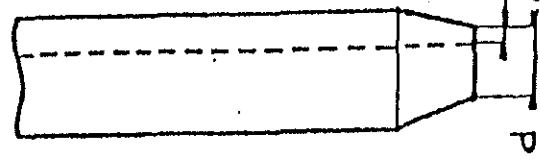
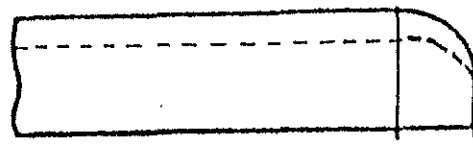
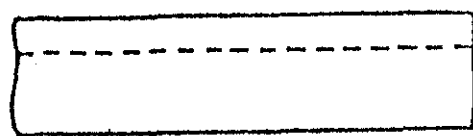
prescribed wake geometry modeling). Thus, it is shown that when the previous code was inefficient to predict the tip vortex path, the calculation made from the new code fits very well the experiments.

Future works based on experiments realised on rotor configurations are planned on the one hand to extend the formulation of radial circulation to non linear twisted blades and evolutive tip shapes ; and on the other hand to validate and improve the free wake analysis calculation of airloads, induced and wake flow fields.

ACKNOWLEDGEMENT : The authors acknowledge the support provided by "Direction des Recherches Etudes et Techniques" under Grant D.R.E.T.n° 84/009.

REFERENCES

- (1) A.J. LANDGREBE : "An analytical and experimental investigation of helicopter rotor hover performance and wake geometry characteristics". AMRDL Technical Report 71-24, June 1971.
- (2) J.D. KOCUREK, J.L. TANGLER : "A prescribed wake lifting surface hover performance analysis". 32nd Annual National Forum of the American Helicopter Society, Washington, D.C., May 1976.
- (3) J.M. POURADIER, E. HOROWITZ : "Aerodynamic study of a hovering rotor". 6th European Rotorcraft and Powered Lift Forum, Bristol, September 1980.
- (4) J.D. BALLARD, K.L. ORLOFF : "Effect of tip shape on blade loading characteristics and wake geometry for a two-bladed rotor in hover". Journal of American Helicopter Society, January 1980.
- (5) M. NSI MBA, C. MEYLAN, C. MARESCA, D. FAVIER : "Radial distribution circulation of a rotor in hover measured by laser velocimeter". Tenth European Rotorcraft Forum. The Hague, August 1984.
- (6) J.M. SUMMA, D.R. CLARK : "A lifting surface method for hover/climb airloads". 35th A.M.S. Forum, Washington, May 1979.
- (7) C. MARESCA, M. NSI MBA, D. FAVIER : "Prédiction et vérification expérimentale du champ des vitesses d'un rotor en vol stationnaire". AGARD CP n°334, Paper N°7, London, May 1982.

Rotor number	Twist	Planform and tip shapes	Profile
1	-8°		BV 23010
2	-14°		BV 23010
3	$-8,3^\circ$ } Non linear		OA 209
4	$-8,3^\circ$	 $\alpha \approx 60^\circ$	OA 209
5	$-8,3^\circ$		OA 209
6	$-8,3^\circ$	 $0,95R \quad R$	OA 209
7	$-8,3^\circ$		OA 209

$$\begin{cases} a = 0,15c \\ b = 0,25c \\ d = 0,60c \end{cases}$$

Figure 1. Experimented rotors

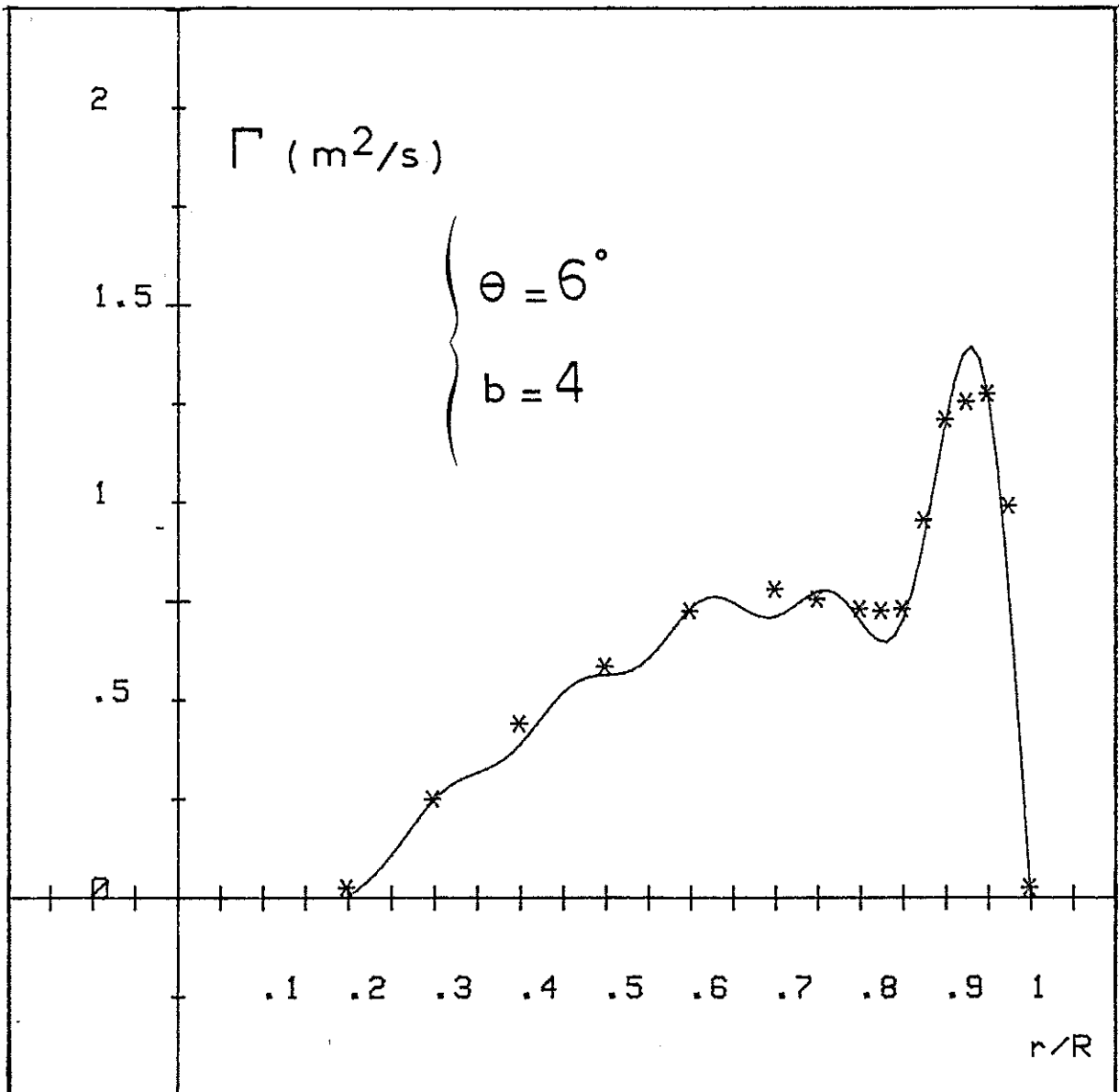


Figure 3. Radial distribution of circulation

* Experiments

— Formula (1)

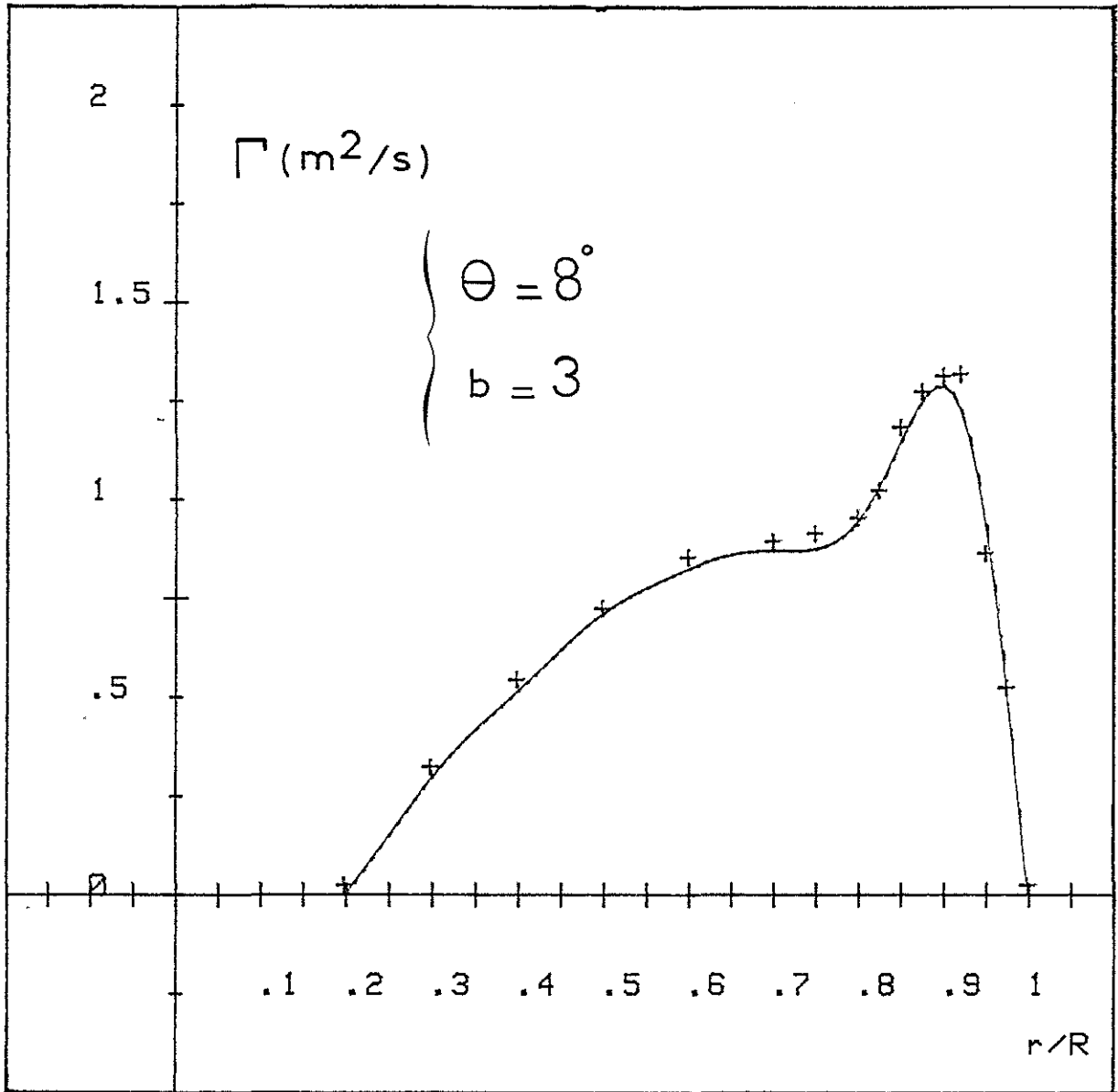


Figure 4. Radial distribution of circulation

+ Experiments

— Formula (1)

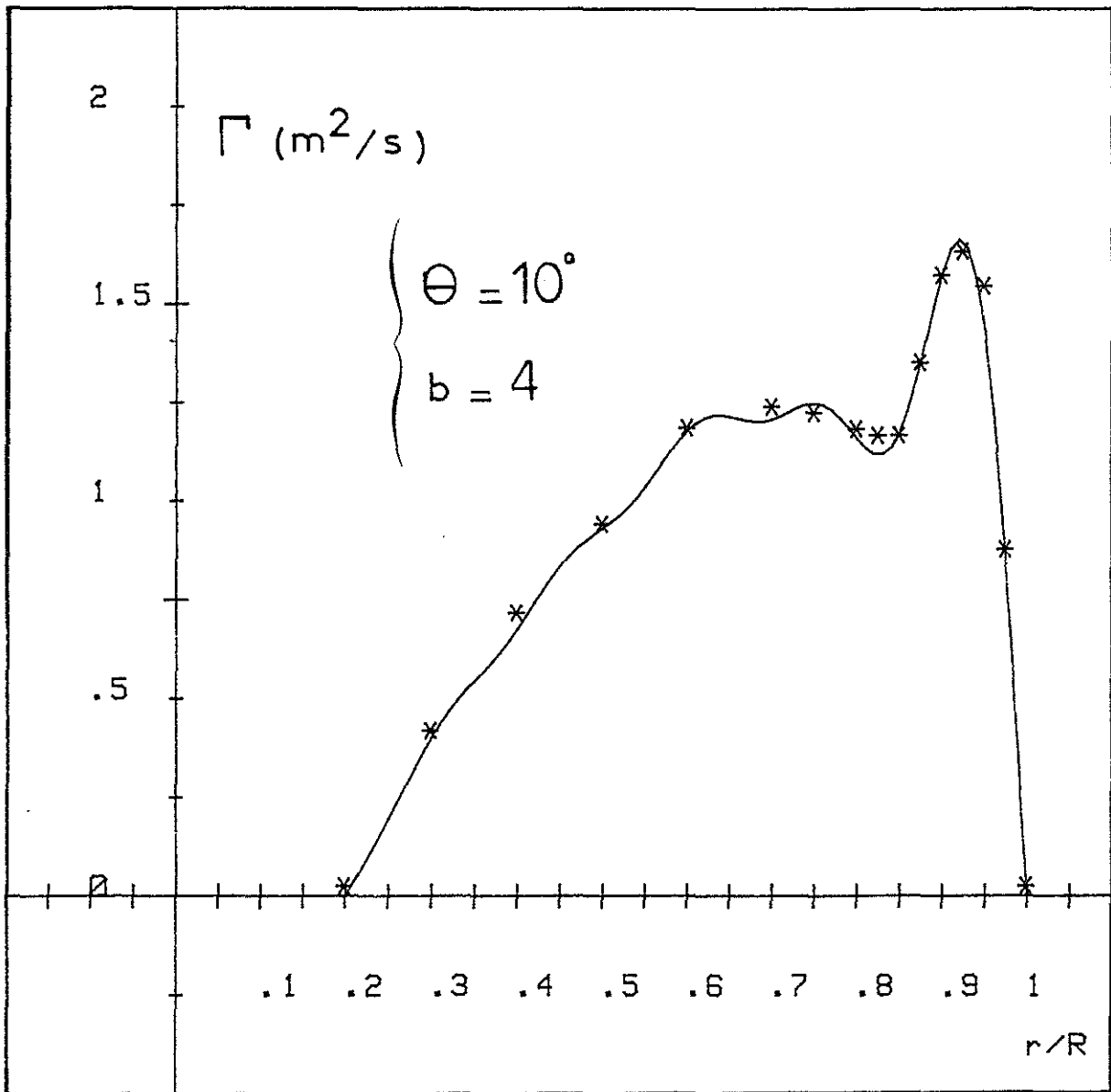


Figure 5. Radial distribution of circulation

* Experiments

— Formula (1)

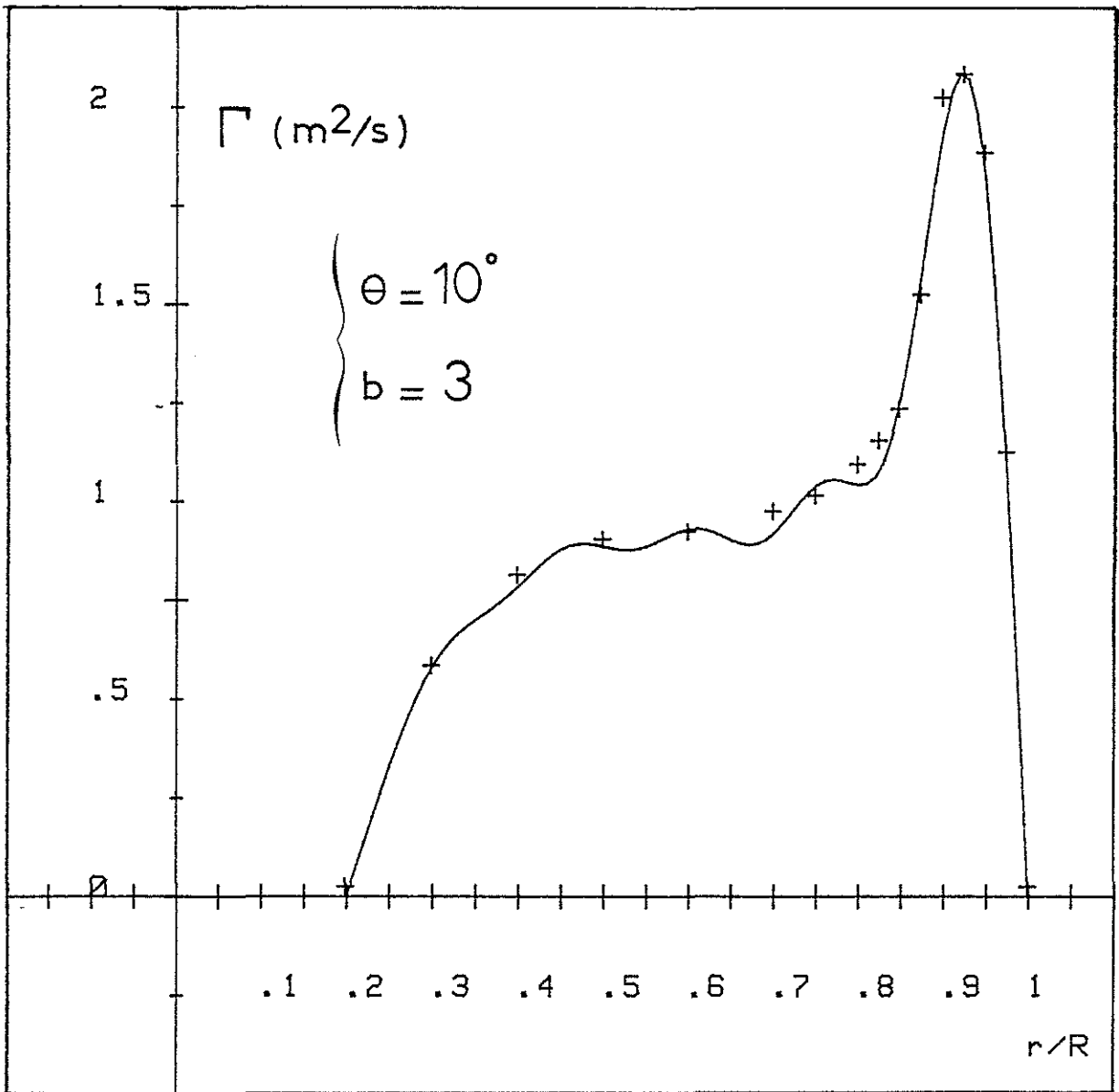


Figure 6. Radial distribution of circulation

+ Experiments

— Formula (1)

INPUT DATA	$b, \sigma, \theta_{0.75}, \theta_v, \Omega, \dots$	$C_L(\alpha, M)$	C_T
------------	---	------------------	-------

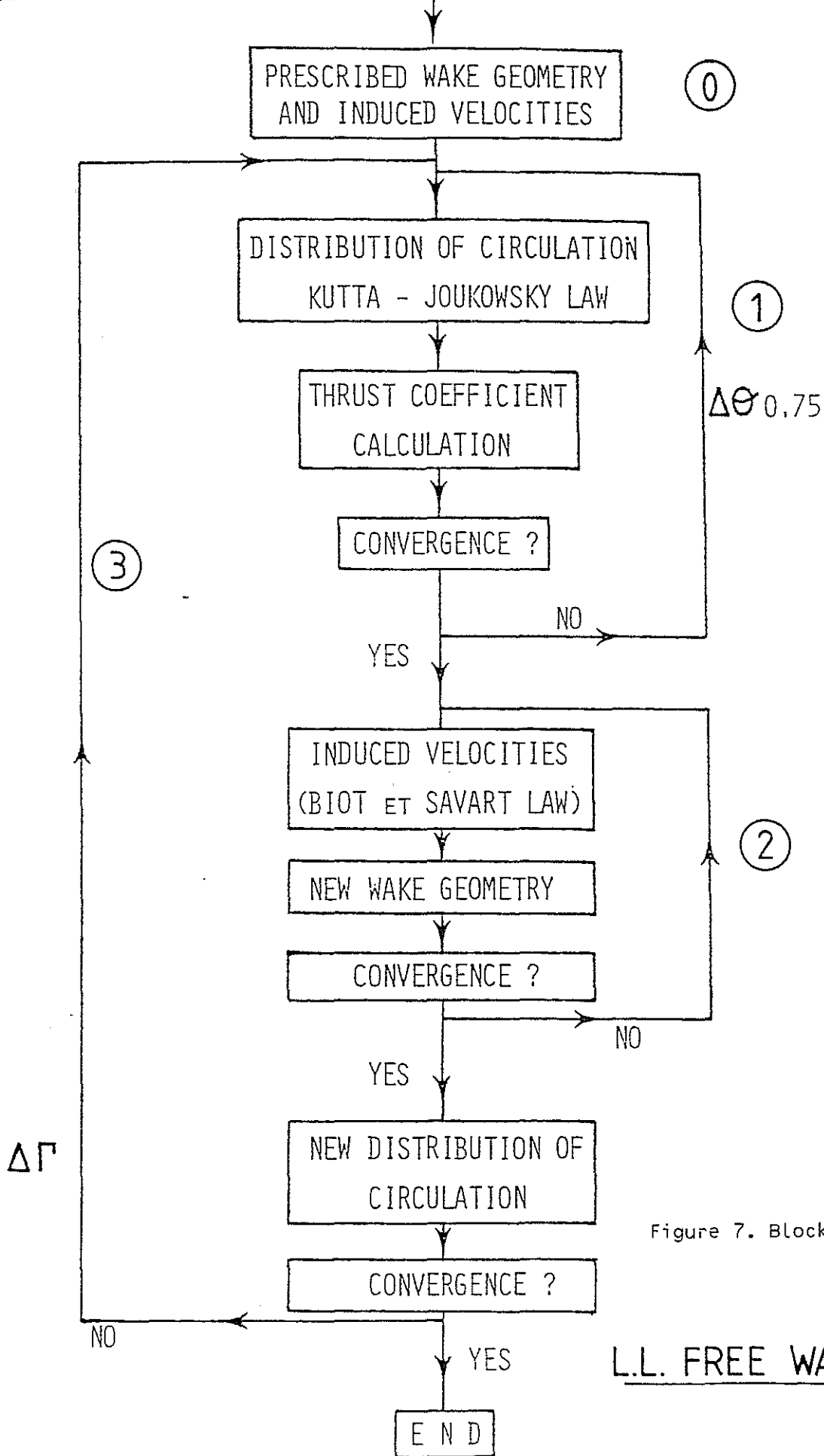


Figure 7. Block-diagram of code 1

L.L. FREE WAKE ANALYSIS

PARAMETERS INFLUENCING THE PREDICTION MODEL

■ Number of calculation points on the blade : N_b

Optimisation as function of b

}	$b=2$	$N_b = 8-11$
	$b=3$	$N_b = 7-8$
	$b=4$	$N_b = 6-7$

■ Tip Vortex core size

Core Radius : $r_t \leq (5/1000) R$

■ Far Wake Geometry

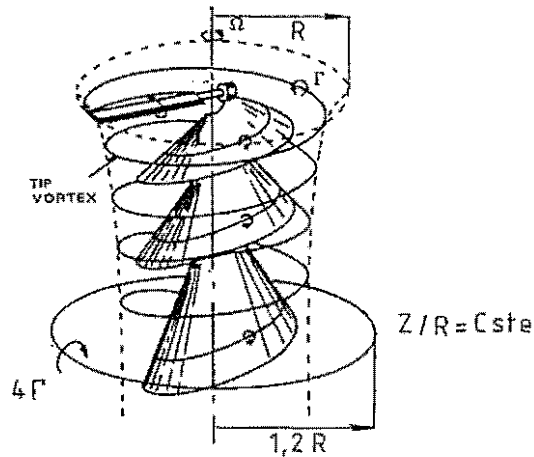


Figure 8. Initial model - Vortex ring

Model a)

Model b) - NEW FAR WAKE MODEL

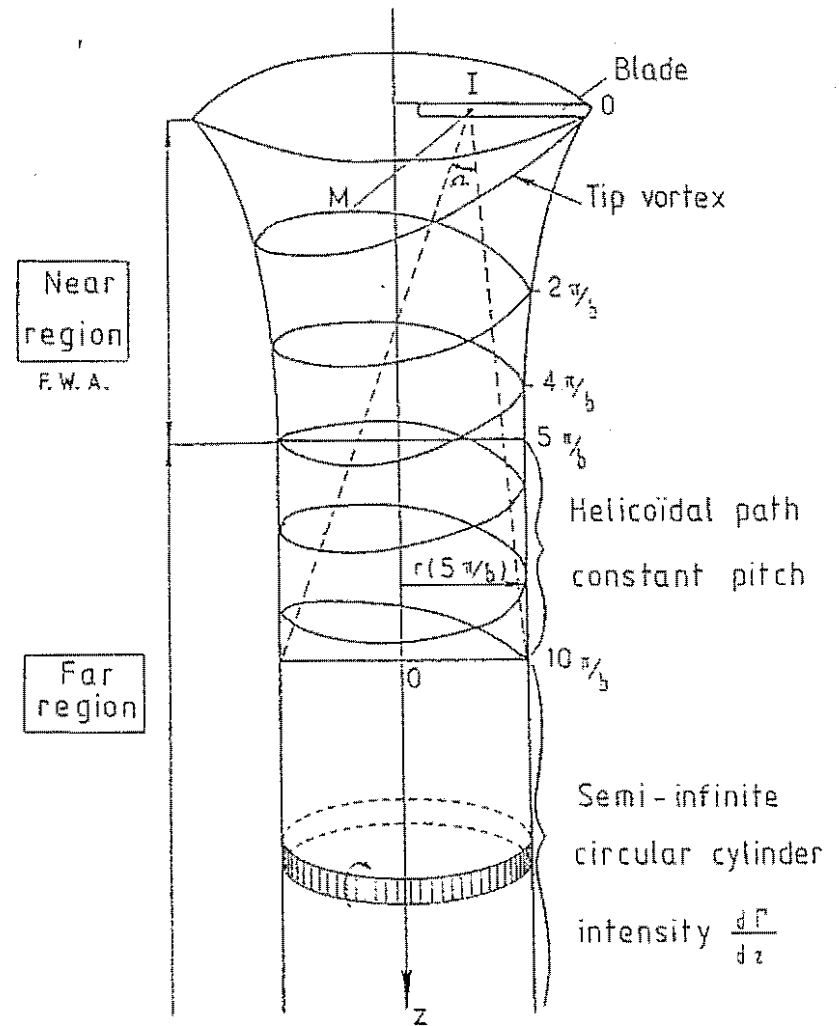


Figure 9

COMPARISON CALCULATION-EXPERIMENT

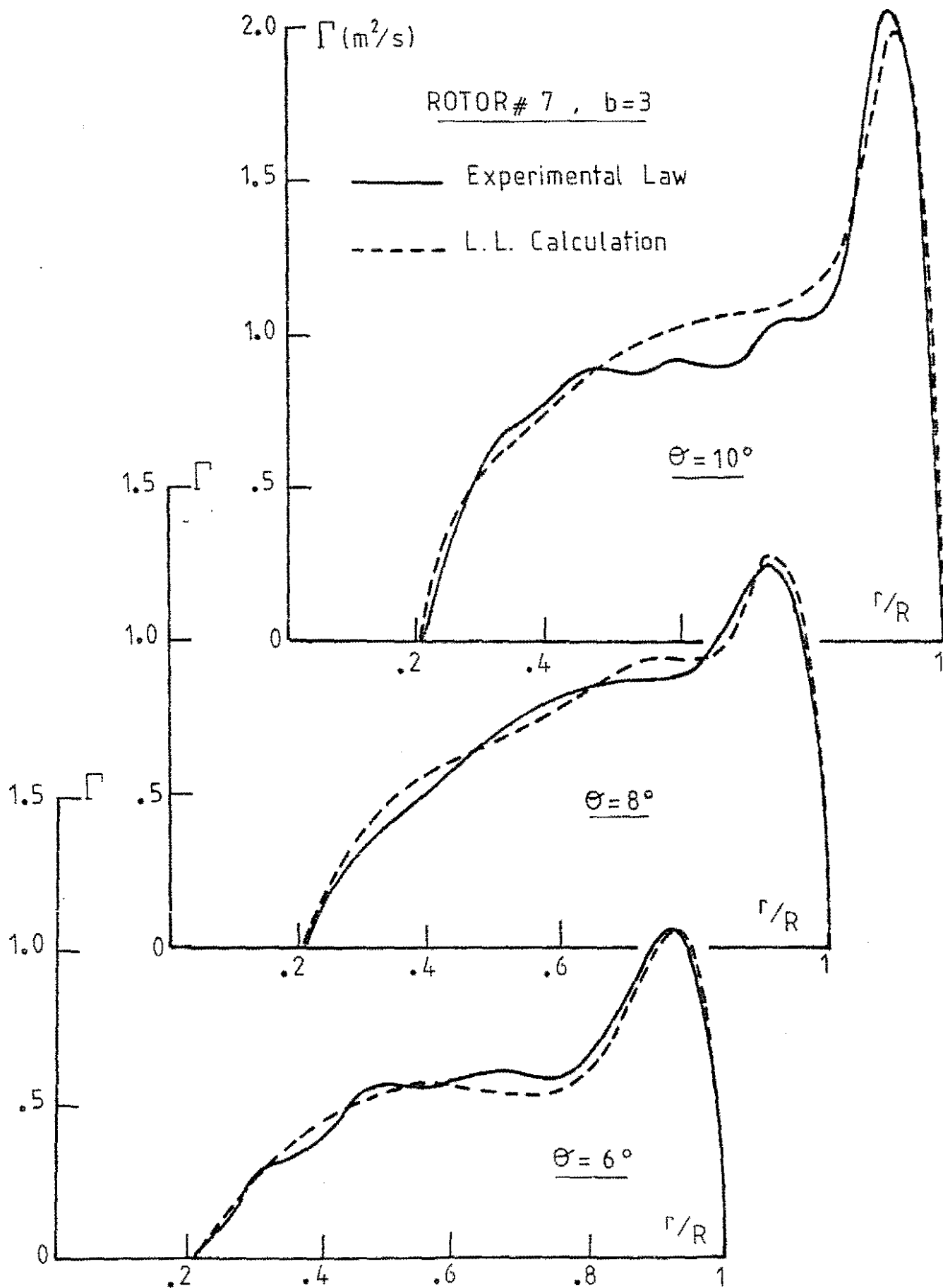


Figure 10

Radial Velocity : \bar{U}

T = 195 N Omega = 134 rd/sec Theta = 10°

Blade Number = 4 Z/R = -.015

Code 1 - - - - - , Code 2 - - - - - , Experiments *

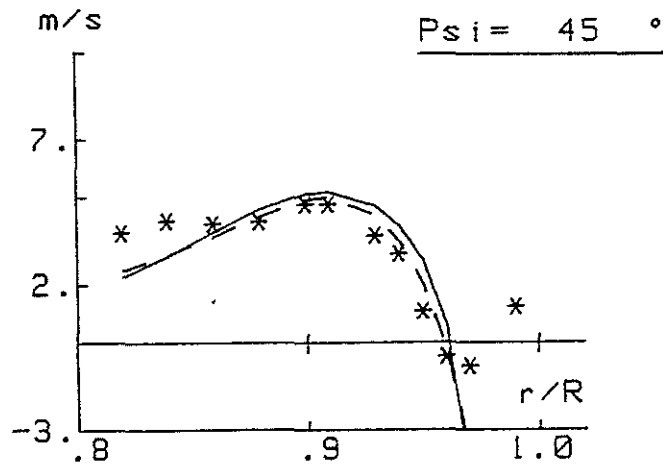


Figure 11

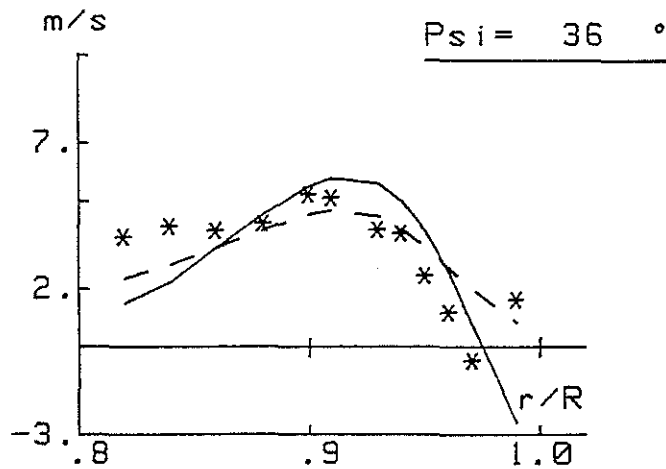


Figure 12

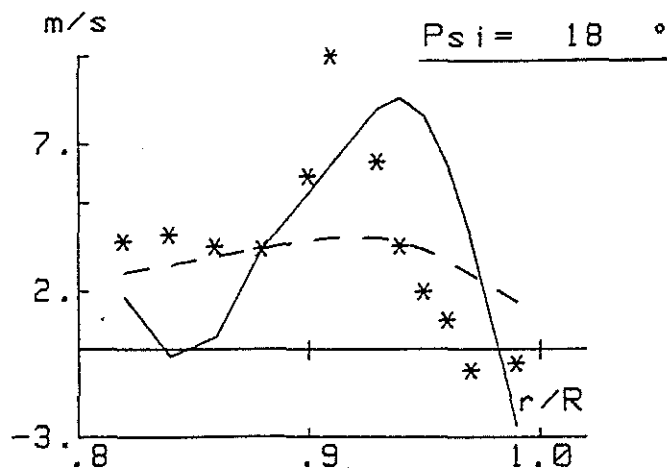


Figure 13

Tangential velocity : V

T = 195 N Omega = 134 rd/sec Theta = 10°

Blade Number = 4 Z/R = -.015

Code 1 - - - - - , Code 2 _____ , Experiments *

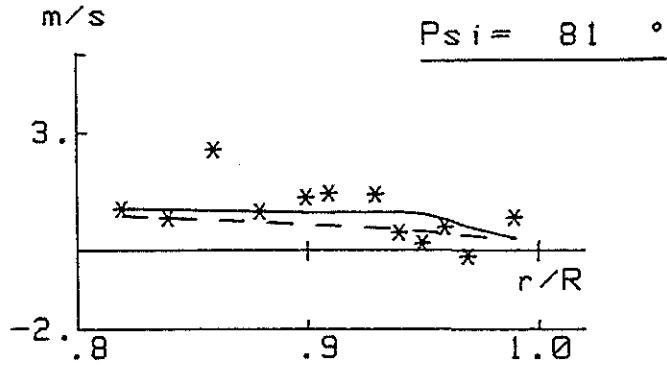


Figure 14

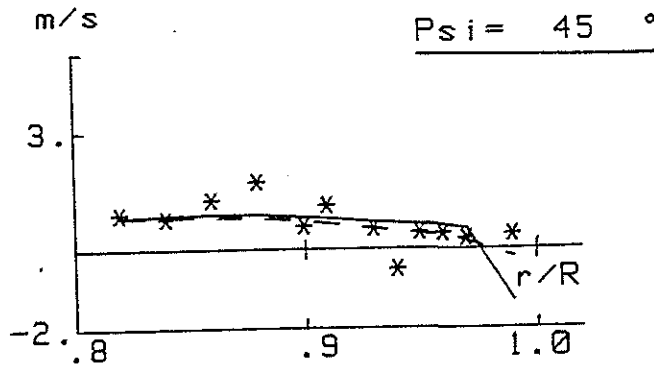


Figure 15

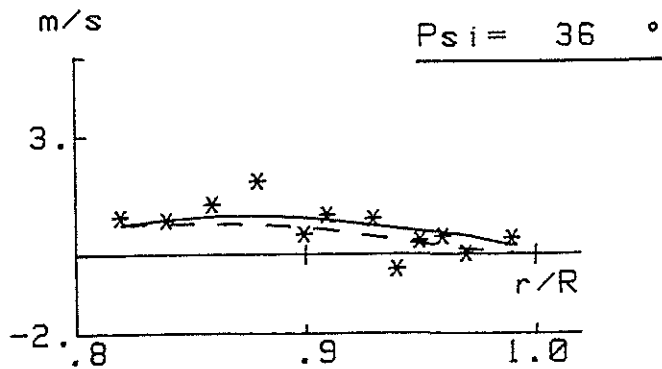


Figure 16

Axial Velocity : W

T = 195 N Omega = 134 rd/sec Theta = 10°

Blade Number = 4 Z/R = -.015

Code 1 - - - - - , Code 2 _____ , Experiments *

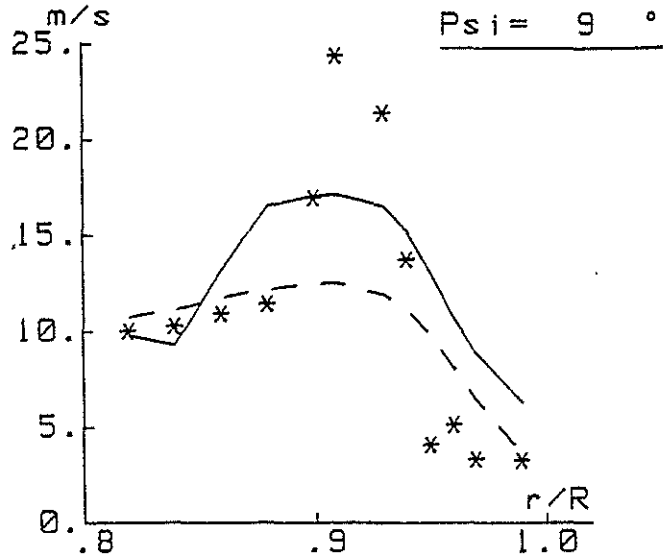


Figure 17

Code 1 - - - - - , Code 2 _____ , Experiments *

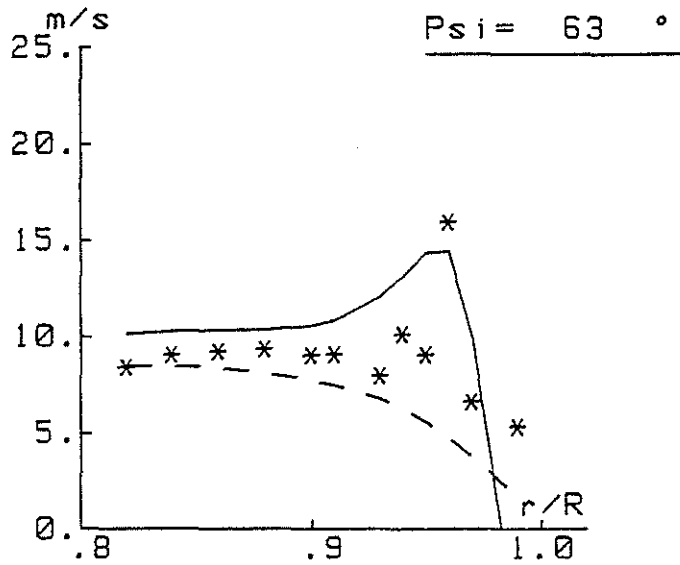


Figure 18

Axial Velocity : W

T = 195 N Omega = 134 rd/sec Theta = 10°

Blade Number = 4 Z/R = -.015

Code 1 - - - - -, Code 2 _____, Experiments *

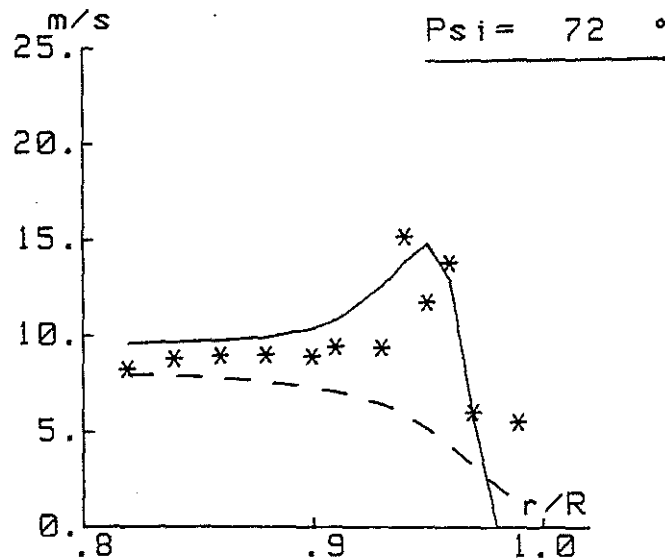


Figure 19

Code 1 - - - - -, Code 2 _____, Experiments *

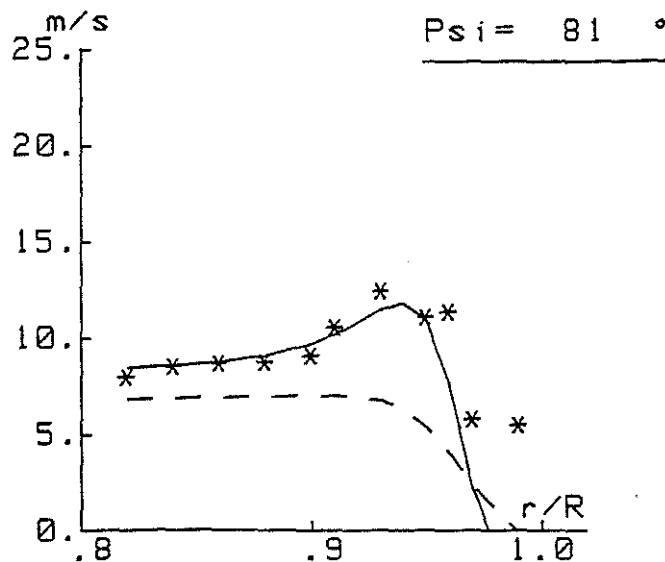


Figure 20

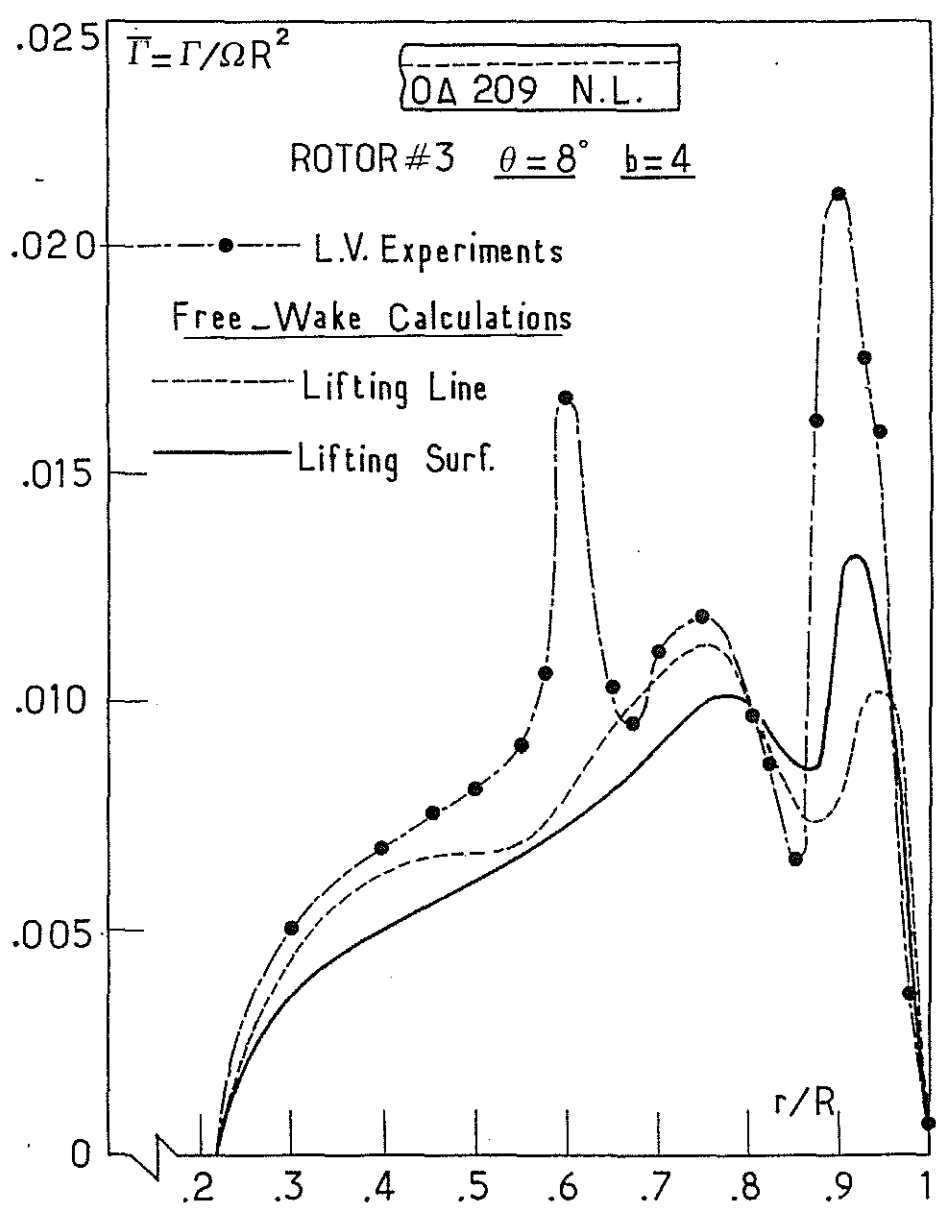
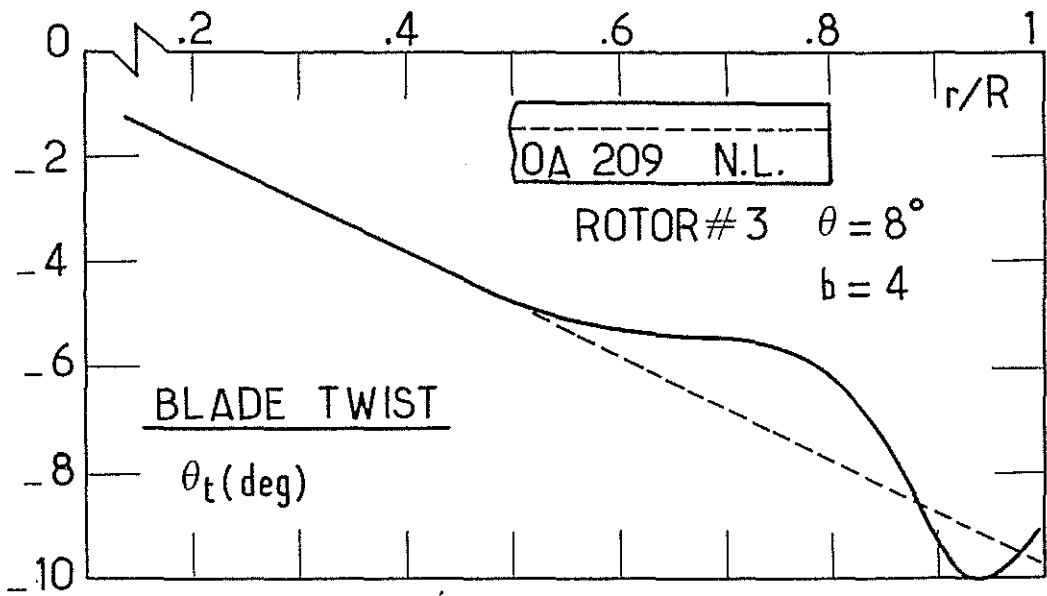


Figure 21 Circulation of a non linear twisted blade.

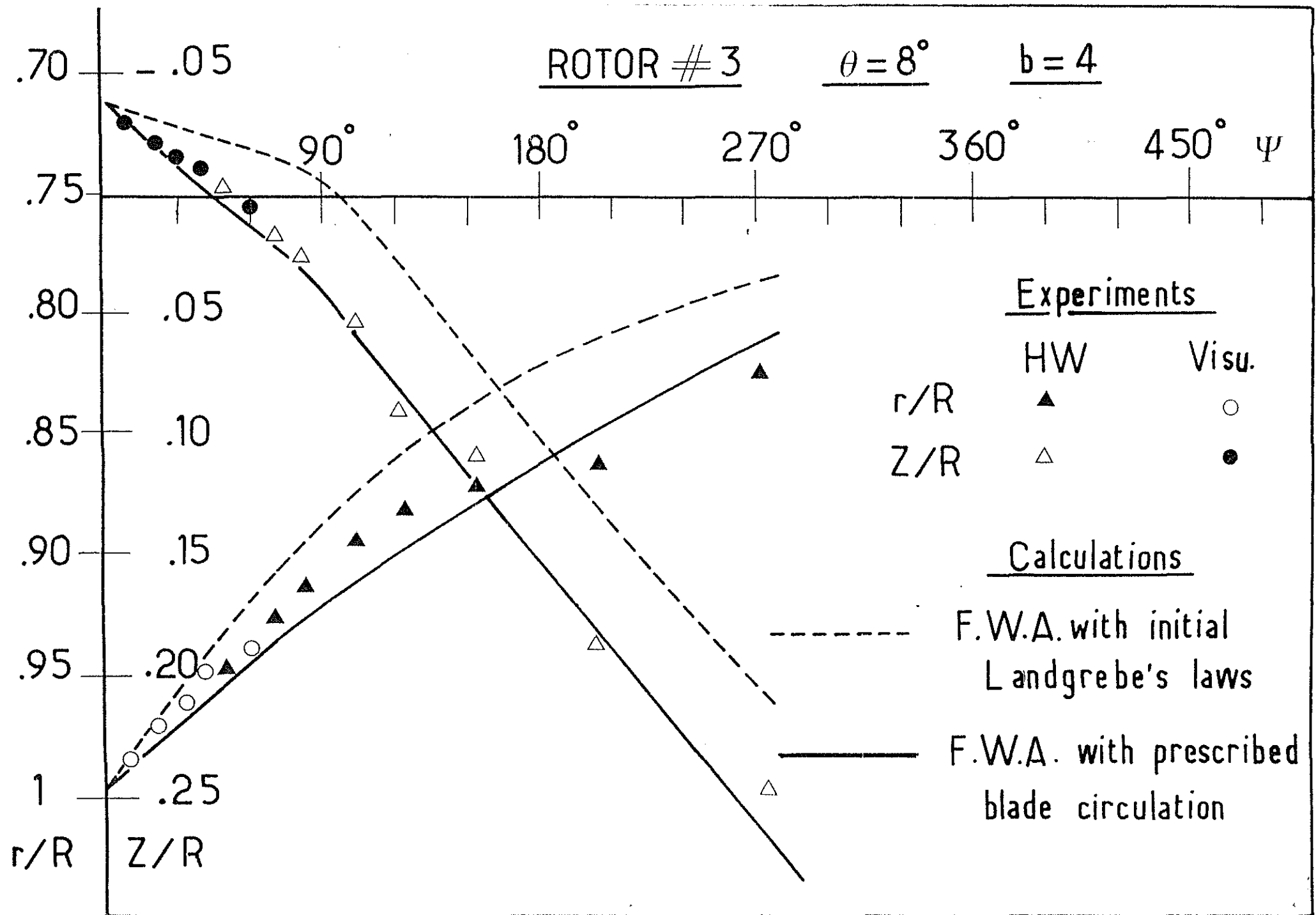


Figure 22. Effect of prescribed circulation on non linear twisted blades.